

# **In-Silico High-Throughput Screening of Ag-Based Electrocatalysts for Anion-Exchange Membrane Fuel Cells**

*Jungwoo Choi<sup>1,§</sup>, Soonho Kwon<sup>1,2,§</sup>, Youngtae Park<sup>1</sup>, Ku Kang<sup>1,3</sup> and Hyuck Mo Lee<sup>1,\*</sup>*

<sup>1</sup>Department of Materials Science and Engineering, KAIST, 291 Daehak-ro, Yuseong-gu, Daejeon 34141, Republic of Korea

<sup>2</sup>Materials and Process Simulation Center (MSC), California Institute of Technology, Pasadena, California 91125, United States

<sup>3</sup>Chemical Biological and Radiological Defense Research Institute, Seoul, Republic of Korea

§: Both authors contributed equally to this work.

\*Corresponding author email: hmlee@kaist.ac.kr

**KEYWORDS: Anion-exchange membrane fuel cells, Oxygen reduction reaction, Ag-based catalyst, Density functional theory, High-throughput screening**

SUPPORTING INFORMATION

Periodic Table of the Elements

	Li	Be										B		N					
	Na	Mg										Al							
		Ca	Sc	Ti						Ni	Cu	Zn		Ge					
		Sr	Y	Zr					Rh	Pd	Ag	Cd	In	Sn	Sb				
		Ba		Hf					Pt	Au	Hg								
		Ra																	
Lanthanide	La	Ce	Pr	Nd	Pm	Sm	Eu	Gd	Tb	Dy	Ho	Er	Tm	Yb	Lu				
Actinide	Ac	Th																	

**Figure S1.** Elements in the Ag-X bimetallic alloys that we explored through high-throughput screening considering various crystal structures based on the Materials Project database. The green elements indicate the X elements of the screened Ag-X bimetallic alloys.

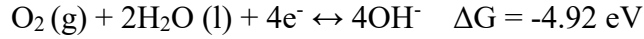
No	Material	Space Group	Crystal Structure	No	Material	Space Group	Crystal Structure
1	Ag <sub>3</sub> Sb	Pmmn	Orthorhombic	54	SrAg <sub>5</sub>	P6/mmm	Hexagonal
2	Ag <sub>3</sub> Sn	Pmmn	Orthorhombic	55	La <sub>3</sub> Ag	P6 <sub>3</sub> /mmc	Hexagonal
3	YbAg	Pnma	Orthorhombic	56	Si <sub>3</sub> Ag	P6 <sub>3</sub> /mmc	Hexagonal
4	AlAg <sub>2</sub>	Cmcm	Orthorhombic	57	ReAg <sub>3</sub>	P6 <sub>3</sub> /mmc	Hexagonal
5	CaAg	Cmcm	Orthorhombic	58	AgAu <sub>3_2a</sub>	P6 <sub>3</sub> /mmc	Hexagonal
6	CaAg <sub>2</sub>	Imma	Orthorhombic	59	AgSe	F-43m	Cubic
7	NdAg <sub>2</sub>	Imma	Orthorhombic	60	AgO	F-43m	Cubic
8	PrAg <sub>2</sub>	Imma	Orthorhombic	61	AgN	F-43m	Cubic
9	SrAg <sub>2</sub>	Imma	Orthorhombic	62	AgC_1	F-43m	Cubic
10	YbAg <sub>2</sub>	Imma	Orthorhombic	63	InAg <sub>3</sub>	Pm-3m	Cubic
11	LuAg <sub>4</sub>	I4/m	Tetragonal	64	ZnAg <sub>3</sub>	Pm-3m	Cubic
12	ScAg <sub>4</sub>	I4/m	Tetragonal	65	AcAg	Pm-3m	Cubic
13	Ti <sub>2</sub> Ag	I4/mmm	Tetragonal	66	MgAg	Pm-3m	Cubic
14	ErAg <sub>2</sub>	I4/mmm	Tetragonal	67	CdAg	Pm-3m	Cubic
15	TmAg <sub>2</sub>	I4/mmm	Tetragonal	68	PrAg	Pm-3m	Cubic
16	LiAg <sub>3</sub>	I4/mmm	Tetragonal	69	YAg	Pm-3m	Cubic
17	Ag <sub>3</sub> Pd	I4/mmm	Tetragonal	70	DyAg	Pm-3m	Cubic
18	Ag <sub>3</sub> Pd_a	I4/mmm	Tetragonal	71	SmAg	Pm-3m	Cubic
19	Li <sub>3</sub> Ag_1	I4/mmm	Tetragonal	72	HoAg	Pm-3m	Cubic
20	Zr <sub>2</sub> Ag	I4/mmm	Tetragonal	73	TmAg	Pm-3m	Cubic
21	TbAg <sub>2</sub>	I4/mmm	Tetragonal	74	NdAg	Pm-3m	Cubic
22	DyAg <sub>2</sub>	I4/mmm	Tetragonal	75	ScAg	Pm-3m	Cubic
23	Hf <sub>2</sub> Ag	I4/mmm	Tetragonal	76	ErAg	Pm-3m	Cubic
24	ScAg <sub>2</sub>	I4/mmm	Tetragonal	77	TbAg	Pm-3m	Cubic
25	YAg <sub>2</sub>	I4/mmm	Tetragonal	78	AgAu <sub>3_1</sub>	Pm-3m	Cubic
26	HoAg <sub>2</sub>	I4/mmm	Tetragonal	79	YbAg	Pm-3m	Cubic
27	LuAg <sub>2</sub>	I4/mmm	Tetragonal	80	MgAg <sub>3_1</sub>	Pm-3m	Cubic
28	TbAg <sub>3_1</sub>	I4/mmm	Tetragonal	81	LiAg	Pm-3m	Cubic
29	ZrAg <sub>2</sub>	I4/mmm	Tetragonal	82	Ag <sub>3</sub> Pt	Pm-3m	Cubic
30	NaAg <sub>3</sub>	I4/mmm	Tetragonal	83	AgPt <sub>3</sub>	Pm-3m	Cubic
31	NiAg <sub>3</sub>	I4/mmm	Tetragonal	84	Ag <sub>3</sub> Hg	Pm-3m	Cubic
32	Ag <sub>3</sub> P	I4/mmm	Tetragonal	85	InAg	Pm-3m	Cubic
33	UAg <sub>3</sub>	I4/mmm	Tetragonal	86	GaAg	Pm-3m	Cubic
34	Si <sub>3</sub> Ag	I4/mmm	Tetragonal	87	AgHg	Pm-3m	Cubic
35	TcAg <sub>3</sub>	I4/mmm	Tetragonal	88	Ag <sub>3</sub> Ge	Pm-3m	Cubic
36	Ag <sub>3</sub> N	I4/mmm	Tetragonal	89	Zr <sub>3</sub> Ag	Pm-3m	Cubic
37	In <sub>2</sub> Ag	I4/mcm	Tetragonal	90	K <sub>3</sub> Ag	Pm-3m	Cubic
38	Th <sub>2</sub> Ag	I4/mcm	Tetragonal	91	Rb <sub>3</sub> Ag	Pm-3m	Cubic
39	AgH	P6 <sub>3</sub> mc	Hexagonal	92	TmAg <sub>3</sub>	Pm-3m	Cubic
40	AgB <sub>2</sub>	P6/mmm	Hexagonal	93	Ti <sub>3</sub> Ag	Pm-3m	Cubic

<b>41</b>	EuAg <sub>5</sub>	P6/mmm	Hexagonal	<b>94</b>	NiAg <sub>3</sub>	Pm-3m	Cubic
<b>42</b>	BaAg <sub>5</sub>	P6/mmm	Hexagonal	<b>95</b>	BeAg <sub>3</sub>	Pm-3m	Cubic
<b>43</b>	BaAg <sub>2</sub>	P6/mmm	Hexagonal	<b>96</b>	Ag <sub>3</sub> Rh	Pm-3m	Cubic
<b>44</b>	AgN	P6 <sub>3</sub> /mmc	Hexagonal	<b>97</b>	V <sub>3</sub> Ag	Pm-3m	Cubic
<b>45</b>	AgAu <sub>3_2</sub>	P6 <sub>3</sub> /mmc	Hexagonal	<b>98</b>	AgN	Pm-3m	Cubic
<b>46</b>	MgAg <sub>3_2</sub>	P6 <sub>3</sub> /mmc	Hexagonal	<b>99</b>	AgAu <sub>3_1a</sub>	Pm-3m	Cubic
<b>47</b>	CdAg <sub>3</sub>	P6 <sub>3</sub> /mmc	Hexagonal	<b>100</b>	Ag <sub>3</sub> Pt_a	Pm-3m	Cubic
<b>48</b>	AcAg <sub>3</sub>	P6 <sub>3</sub> /mmc	Hexagonal	<b>101</b>	AgPt <sub>3_a</sub>	Pm-3m	Cubic
<b>49</b>	Li <sub>3</sub> Ag_2	P6 <sub>3</sub> /mmc	Hexagonal	<b>102</b>	Ag <sub>3</sub> Hg_a	Pm-3m	Cubic
<b>50</b>	Mg <sub>3</sub> Ag	P6 <sub>3</sub> /mmc	Hexagonal	<b>103</b>	AgN	Fm-3m	Cubic
<b>51</b>	TbAg <sub>3_2</sub>	P6 <sub>3</sub> /mmc	Hexagonal	<b>104</b>	AgC_2	Fm-3m	Cubic
<b>52</b>	CuAg <sub>3</sub>	P6 <sub>3</sub> /mmc	Hexagonal	<b>105</b>	Pt	Fm-3m	Cubic
<b>53</b>	AgPb <sub>3</sub>	P6 <sub>3</sub> /mmc	Hexagonal	<b>106</b>	Ag	Fm-3m	Cubic

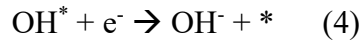
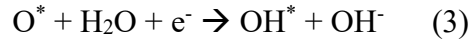
**Table S1.** Materials, space groups, and crystal structures were explored through high-throughput screening considering various crystal structures. AB, AB\_1 and AB\_2 denote materials with the same composition but different space groups. AB\_a denotes materials that are modeled as a AgX skin due to the high dissolution potential of the X atom.

## Thermodynamic overpotential calculations

The oxygen reduction reaction (ORR) forms  $4\text{OH}^-$  from molecular oxygen  $\text{O}_2$ ,  $\text{H}_2\text{O}$  and electrons.



The  $4\text{e}^-$ -transfer oxygen reduction reaction mechanism is composed of four steps:



The conditions were  $T = 300 \text{ K}$ ,  $\text{pH} = 14$ ,  $P_{\text{H}_2\text{O}} = 0.035 \text{ bar}$  and  $P_{\text{O}_2} = 1 \text{ bar}$ . Under these conditions,  $\text{H}_2\text{O}(\text{g})$  and  $\text{H}_2\text{O}(\text{l})$  were in thermodynamic equilibrium, and we used the following assumptions to calculate the overpotential.<sup>1,2</sup>

Assumption S1: Computational hydrogen electrode



Assumption S2: Corrections for entropy, zero-point vibrations, solvation and coverage effects

$$\Delta G_{\text{O}^*} = \Delta E_{\text{O}^*} + 0.01 \text{ eV}$$

$$\Delta G_{\text{OH}^*} = \Delta E_{\text{OH}^*} - 0.25 \text{ eV}$$

Assumption S3: Scaling relation

$$\Delta G_{\text{OOH}^*} = \Delta G_{\text{OH}^*} + 3.2 \text{ eV}$$

As a result, the Gibbs free energy changes for each step were calculated using the following equations (S1-S4):

$$\Delta G_1(U) = \Delta E_{\text{OH}^-} - 1.97 + U \quad (\text{S1})$$

$$\Delta G_2(U) = \Delta E_O - \Delta E_{OH} - 2.94 + U \quad (S2)$$

$$\Delta G_3(U) = \Delta E_{OH} - \Delta E_O - 0.26 + U \quad (S3)$$

$$\Delta G_4(U) = U - \Delta E_{OH} + 0.25 \quad (S4)$$

The activity (-overpotential) was calculated by means of the following equation:

$$\text{Activity} = - \max [\Delta G_1(U), \Delta G_2(U), \Delta G_3(U), \Delta G_4(U)]$$

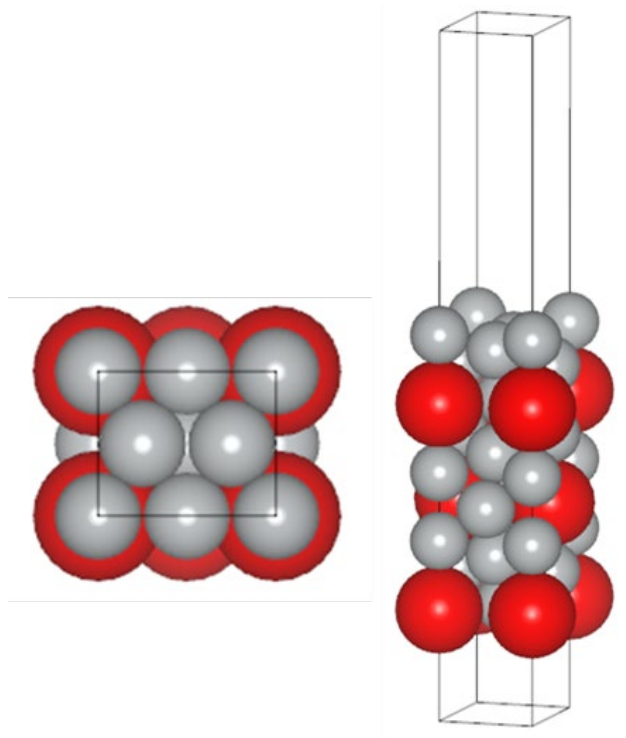


**Figure S2.** Structure of  $XAg_5$  with  $P6/mmm$  (hexagonal) ( $X= Ba, Sr$  and  $Eu$ ), which were the candidates proposed after high-throughput screening. The red atoms represent  $Ba, Sr$  or  $Eu$ , and the gray atoms represent  $Ag$ .